Mechanism and Machine Theory 109 (2017) 296–312

Contents lists available at ScienceDirect

Mechanism and Machine Theory

journal homepage: www.elsevier.com/locate/mechmachtheory

Research paper

Design of planar variable-payload balanced articulated manipulators with actuated linear ground-adjacent adjustment

Wei-Hsuan Chiang, Dar-Zen Chen*

Department of Mechanical Engineering, National Taiwan University, No. 1, Sec. 4, Roosevelt Road, Taipei 10617, Taiwan (R.O.C.)

ARTICLE INFO

Keyword:
Variable payload
Balanced
Spring
Ground
Adjustment

ABSTRACT

Supporting different payloads has been shown to be effective for developing a multitasking manipulator. This paper presents a method for designing a planar, statically balanced, articulated manipulator for supporting variable payloads. The balancing equations for the gravitational and spring elastic energies are developed using a stiffness block matrix, which represents interacting potential energies between the links. It is shown that the springs can be classified according to the roles they play in the balancing equations. Thus, the installation parameters can be divided into payload-dependent parameters (PDPs) and payload-independent parameters (PIPs). The admissible spring configurations for supporting variable payloads are determined using the required number of PDPs, and PDP adjustment devices are used to adjust PDPs as the payload changes. Based on the interrelation between PDPs and PIPs, the number of PDPs can be reduced through proper arrangement of PIPs. The displacement of different PDPs can be equalized to fit attachment points in the same adjustment device. Therefore, the number of PDP adjustment devices is minimized to one. Variable-payload balanced articulated manipulators with five springs and three degrees of freedom are shown as illustrative examples. The energy consumption is estimated accordingly.

1. Introduction

Statically balanced manipulators maintain equilibrium in any configuration. In recent years, several methodologies have been proposed to compensate for the weight of linkages. One such method is the counterweight method that balances a manipulator by supplying counterweights that cancel out the effect of link mass; however, this increases the system's inertia, and the operation may be worsened [1–4]. Another method is the spring-balancing method that uses spring forces to compensate for gravitational forces; consequently, the system's inertia remains small [5–10].

One of the spring-balancing approaches is to use auxiliary linkages. The method of parallelogram links ensures that vertical members exist at the end of each link. Therefore, a manipulator with multiple degrees of freedom (DOF) can be considered as a series of connected 1-DOF manipulators [11–14]. Agrawal et al. applied auxiliary parallelograms to human upper arm orthotic devices [15], human leg orthotic devices [16], and assistive devices for sit-to-stand tasks [17] to support people experiencing muscle weakness. This method can be further applied to spatial parallel platform mechanisms [18–21], and delta robots [22,23] to enhance their low-dynamic performance levels. However, auxiliary linkages tend to increase the inertia of the system. Also, the range of motion may be limited. For the improvement of these problems, Lin et al. proposed a stiffness block matrix (SBM) to explore the potential energies interacting between links of multiple-link planar articulated manipulators [24–26]. Those interacting potential

* Corresponding author.
E-mail address: dzchen@ntu.edu.tw (D.-Z. Chen).

http://dx.doi.org/10.1016/j.mechmachtheory.2016.12.001
Received 13 May 2016; Received in revised form 15 November 2016; Accepted 1 December 2016

energies can be compensated by various approaches without auxiliary linkages. Although the configurations of springs may be relatively complex, the locations at which those springs must be installed can be derived easily. Therefore, the aim of this paper is to determine the location of the springs.

With the increasing usage of support or assistive equilibrators, supporting variable payloads has been shown to be effective for multitasking manipulators, such as robotic arms, surgical light assistance devices, and monitor support devices. Therefore, balanced devices that support variable payloads have been developed. To maintain static balance, the spring configuration should be altered for different payloads. Nathan proposed a static balancer in which spring attachment points can be self-adjusted [27]. Herder et al. proposed several energy-free adjusting concepts such as virtual springs [28], simultaneous displacement [29], spring stiffness [30], and storage springs [31]. Takesue et al. focused on the spring configuration of variable gravity compensation mechanisms. Two types of springs with a 90° phase difference can be used to compensate for variation in gravity without using wires [32]. Energy-free design is not a major concern in this context; adjustments may consume energy, some extra energy may be allowed into the system during the adjustment of the attachment points. However, these methods are focused on the compensation of gravitational and elastic forces between ground and ground-adjacent links. Information about interacting potential energies between multiple links is not sufficient. The designs of the auxiliary linkages may require alterations to adapt them to the needs of a multiple-link manipulator. Therefore, this paper focuses on the spring configuration of multiple-link planar articulated manipulators and estimation of the energy consumption during adjustment.

The method proposed in this paper is based on the SBM approach [24]. Previous studies of the SBM approach [24–26] have mainly focused on the compensation of fixed gravitational potential energy. In the present paper, however, the SBM approach is generalized for variable payloads. The adjustable installation parameters in the balancing equations, which must vary with the changes of the payload, are called payload-dependent parameters (PDPs). By contrast, the installation parameters for fixed locations are defined as payload-independent parameters (PIPs). The process of this paper is roughly summarized as follows. On the basis of the interrelation between the PDPs and the PIPs, the displacement of the PDPs can be expressed as a linear equation and the number of PDPs can be reduced through the proper arrangement of associated PIPs. Therefore, the PDP adjustment device can be implemented as a slider that can lock at any position along a perpendicular slide rail. Furthermore, all PDPs can be fitted on the same PDP adjustment device to minimize the required number of adjustment devices to one. The energy consumption during the adjustment is estimated based on the simulation results of the variation of total potential energy for a variable payload.

The remainder of this paper is organized as follows. Section 2 introduces the formulations of the elastic potential energy and gravitational potential energy represented by the SBM. On the basis of the summation of the gravitational and elastic SBMs, the spring installation parameters are classified according to the roles they play in the balancing equations. Section 3 describes the general criteria for admissible spring configurations for an n-link variable-payload manipulator (VPM). According to the number of required PDPs, balancing equations are derived from the nonzero component matrices of the summation of the gravitational and elastic SBMs. The formulation of the PDPs and PIPs is then explored according to the spring configuration. Section 4 expresses the displacement terms of the PDPs as an equation in terms of the PIPs. Some additional criteria for the installation of PIPs are determined to reduce and equalize the nonzero displacement PDPs. Section 5 presents the derivation of a planar 3-DOF VPM with five springs as a design example. The static equilibrium of quasistatic continuous motion is verified, and the energy consumption is estimated accordingly.

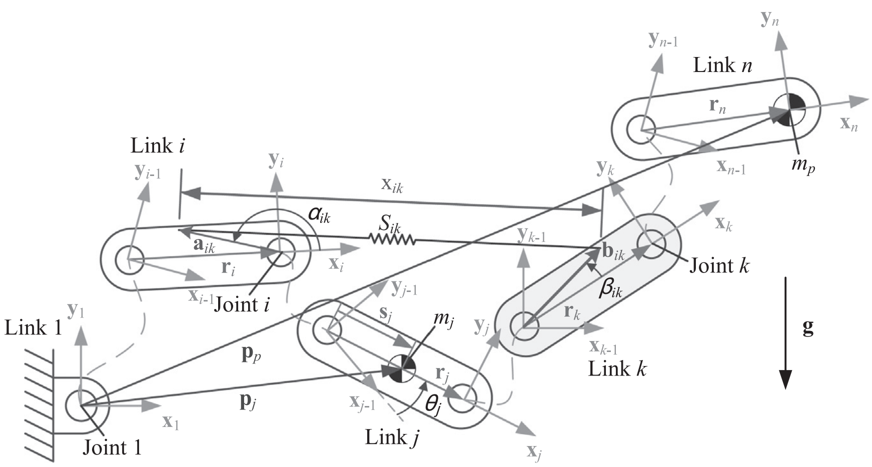

Fig. 1. Center of gravity position $\mathbf{p}_j$ of the n-link planar articulated manipulator and changeable payload fitted at the end effector of link n and S_{ik}, the spring connected between link i and link k.

2. Characteristics of SBM

2.1. SBM

The coordinate system is defined in the Denavit-Hartenberg representation, shown in Fig. 1. The term $\mathbf{r}_j$ denotes the direction vector of link j of an n-link manipulator. The terms $\mathbf{x}_j$ and $\mathbf{y}_j$ are unit orthonormal axis vectors, where $j = 1, 2, ..., n$. The terms $\mathbf{r}_j$, $\mathbf{x}_j$, and $\mathbf{y}_j$ are defined to be 2×1 column matrices for 2D space. $\mathbf{R}(\theta_j)$ represents the rotation matrix of the succeeding and preceding coordinate systems, where θ_j is the joint angle from the $\mathbf{x}_{(j-1)}$ axis to the $\mathbf{x}_j$ axis. Therefore, the change in the succeeding coordinate system can be determined according to the rotation of the preceding link.

2.1.1. Characteristics of gravitational SBM

The SBM method was proposed in previous studies for analyzing a statically balanced articulated manipulator with fixed potential energy [24,26]. The term m_j represents the mass of link j; $\mathbf{p}_j$ represents the position vector of the center of mass aligned along the line passing through the joints of links; and $\mathbf{g}$ represents the gravitational acceleration; $\mathbf{I}'$ represents the rotation matrix that rotates 270°. The gravitational potential energy U^g is expressed as

$$U^g = -\sum_{j=2}^{n} m_j \mathbf{g}^{\mathbf{T}} \mathbf{p}_j \tag{1}$$

where

$$\mathbf{p}_j = \mathbf{s}_j + \textstyle\sum_{v=1}^{j-1} \mathbf{r}_v = \frac{s_j}{r_j}\mathbf{r}_j + \sum_{v=1}^{j-1} \mathbf{r}_v \quad j = 2, \ \ldots, \ n \tag{2a}$$

$$\mathbf{g} = g\mathbf{R}\left(\frac{3\pi}{2}\right)\mathbf{x}_1 = g\begin{bmatrix} 0 & -1 \\ 1 & 0 \end{bmatrix}\mathbf{x}_1 = g\mathbf{I}'\mathbf{x}_1 \tag{2b}$$

where $\mathbf{r}_j$ is the direction vector of link j, and $\mathbf{s}_j$ is the vector from joint $(j-1)$ to the center of mass of link j, and its orientation is the same as that of direction vector $\mathbf{r}_j$. In addition, r_j and s_j are the magnitudes of $\mathbf{r}_j$ and $\mathbf{s}_j$, respectively.

In this study, variable payloads are embedded at the end effector of the articulated manipulator. Therefore, the gravitational potential energy consists of the sum of the gravitational energy values of links and variable payloads. The term m_p represents the mass of the payload, which is variable; and $\mathbf{p}_p$ represents the position vector of the variable payload fitted at the end effector of link n. The gravitational potential energy U^g is rearranged as

$$U^g = -m_p \mathbf{g}^{\mathbf{T}} \mathbf{p}_p - \sum_{j=2}^{n} m_j \mathbf{g}^{\mathbf{T}} \mathbf{p}_j \tag{3}$$

where

$$\mathbf{p}_p = \sum_{v=1}^{n} \mathbf{r}_v \tag{4}$$

According to Eqs. (1–4), the SBM representation for the gravitational potential energy can be obtained as

$$U^g = \frac{1}{2}\sum_{v=1}^{n} (\mathbf{r}_1{}^T \mathbf{G}_{1v} \mathbf{r}_v + \mathbf{r}_v{}^T \mathbf{G}_{v1} \mathbf{r}_1) = \frac{1}{2}\begin{bmatrix} \mathbf{x}_1 \\ \mathbf{r}_2 \\ \vdots \\ \mathbf{r}_n \end{bmatrix}^{\mathbf{T}} [\mathbf{G}_{uv}] \begin{bmatrix} \mathbf{x}_1 \\ \mathbf{r}_2 \\ \vdots \\ \mathbf{r}_n \end{bmatrix} \tag{5}$$

where $[\mathbf{G}_{uv}]$ is called the gravitational SBM, and its elements $\mathbf{G}_{uv}$ are called gravitational component matrices, which represent gravitational potential energies interacting between links u and v. Owing to its symmetry [18], $\mathbf{G}_{uv}$ can be expressed as an SBM, as shown in Eq. (6), and only the upper triangular matrix is considered.

$$[\mathbf{G}_{uv}] = \begin{bmatrix} 0 & \mathbf{G}_{12} & \cdots & \mathbf{G}_{1v} & \cdots & \mathbf{G}_{1n} \\ & 0 & 0 & \cdots & \cdots & 0 \\ & & \ddots & & & \vdots \\ & & & \ddots & & \vdots \\ & & & & \ddots & 0 \\ & & & & & 0 \end{bmatrix} \tag{6}$$

The gravitational component matrices $\mathbf{G}_{1v}$ are expressed as

$$\mathbf{G}_{1v} = -g(m_p + W_v)\mathbf{I}' = -g\left(m_p + m_v \frac{s_v}{r_v} + \textstyle\sum_{j=v+1}^{n} m_j\right)\mathbf{I}' \quad v = 2, \ \ldots, \ n \tag{7}$$

where W_v is the sum of the masses of links from v to n. Each component matrix $\mathbf{G}_{uv}$ in the gravitational SBM represents the quantity of the gravitational effect that acts between the ground (link 1) and link v.

2.1.2. Characteristics of elastic SBM

The spring configuration matrix $[S_{ik}]$ represents the configuration of fitted springs in an n-link SBM. S_{ik} = 0 denotes that there is no spring installed between links i and k, and S_{ik} = # (for # ≠ 0) denotes that at least one spring is installed between links i and k.

The expression of elastic potential energy was suggested by Lee et al.[24]. A zero-free-length spring with spring constant k_{ik}, fitted between links i and k of an n-link articulated manipulator, is shown in Fig. 1 as S_{ik}. Assume that the springs used are zero-free-length springs, and the distance between two attachment points $|\mathbf{x}_{ik}|$ can be considered the elongation of the spring. The elastic potential energy can be expressed as

$$U^{ik} = \frac{1}{2}k_{ik}\mathbf{x}_{ik}{}^T\mathbf{x}_{ik} \tag{8}$$

where

$$\mathbf{x}_{ik} = \mathbf{b}_{ik} - \mathbf{a}_{ik} + \sum_{u=i+1}^{k-1}\mathbf{r}_u \tag{9}$$

$\mathbf{a}_{ik}$ and $\mathbf{b}_{ik}$ are proximal and distal installation parameters, respectively. Their position vectors extend from the joints of links i and k, respectively, to the attachment points of the spring, and they can be expressed as

$$\mathbf{a}_{ik} = \begin{cases} \frac{a_{1k}}{x_1}\mathbf{R}(\alpha_{1k})\mathbf{x}_1 = a_{1k}\mathbf{R}(\alpha_{1k})\mathbf{x}_1 & i = 1 \\ \frac{a_{ik}}{r_i}\mathbf{R}(\alpha_{ik})\mathbf{r}_i & i \neq 1 \end{cases} \tag{10a}$$

$$\mathbf{b}_{ik} = \frac{b_{ik}}{r_k}\mathbf{R}(\beta_{ik})\mathbf{r}_k \tag{10b}$$

where $\mathbf{R}(\alpha_{ik})$ and $\mathbf{R}(\beta_{ik})$ are 2×2 rotation matrices, and α_{ik} and β_{ik} are the attachment angles from $\mathbf{r}_i$ to $\mathbf{a}_{ik}$ and from $\mathbf{r}_k$ to $\mathbf{b}_{ik}$, respectively. Note that for the special case for springs with i = 1, as shown in Eq. (10a), x_1 is the length of unit vector $\mathbf{x}_1$, hence, it equal to 1. According to Eq. (8–10), the SBM representation for the elastic potential energy can be obtained as

$$U^{ik} = \frac{1}{2}\sum_{u,v=1}^{n}\mathbf{r}_u{}^T\mathbf{K}_{1v}^{ik}\mathbf{r}_v = \frac{1}{2}\begin{bmatrix}\mathbf{x}_1\\ \mathbf{r}_2\\ \vdots\\ \mathbf{r}_n\end{bmatrix}^T[\mathbf{K}_{uv}^{ik}]\begin{bmatrix}\mathbf{x}_1\\ \mathbf{r}_2\\ \vdots\\ \mathbf{r}_n\end{bmatrix} \tag{11}$$

where $[\mathbf{K}_{\mathrm{uv}}^{\mathrm{ik}}]$ is called the elastic SBM of spring S_{ik}, and the elements $\mathbf{K}_{\mathrm{uv}}^{\mathrm{ik}}$ are called elastic component matrices, which represent elastic interacting potential energies between links u and v. Because $[\mathbf{K}_{\mathrm{uv}}^{\mathrm{ik}}]$ is a symmetric matrix, only the upper triangular matrix is considered as represented in the following:

$$[\mathbf{K}_{uv}^{ik}] = \begin{bmatrix} \mathbf{0} & & \cdots & & \mathbf{0} \\ & \mathbf{K}_{ii}^{ik} & \cdots & \mathbf{K}_{iv}^{ik} & \cdots & \mathbf{K}_{ik}^{ik} & \\ & & \ddots & \mathbf{K}_{uv}^{ik} & \cdots & \mathbf{K}_{uk}^{ik} & \\ & & & \ddots & & \vdots & \vdots \\ & & & & \ddots & \vdots & \\ & & & & & \mathbf{K}_{kk}^{ik} & \\ & & & & & & \mathbf{0} \end{bmatrix} \tag{12}$$

The off-diagonal terms of the elastic component matrices $\mathbf{K}_{\mathrm{uv}}^{\mathrm{ik}}$ (for $u \neq v$) are expressed as

$$\mathbf{K}_{uv}^{ik} = \begin{cases} -k_{ik}\frac{a_{ik}}{r_i}\mathbf{R}(-\alpha_{ik}) & u = i;\quad v = i+1,\ \ldots,\ k-1 \\ -k_{ik}\frac{a_{ik}}{r_i}\frac{b_{ik}}{r_k}\mathbf{R}(\beta_{ik} - \alpha_{ik}) & u = i;\quad v = k \\ k_{ik}\mathbf{I} & u,\quad v = i+1,\ \ldots,\ k-1 \\ k_{ik}\frac{b_{ik}}{r_k}\mathbf{R}(\beta_{ik}) & u = i+1,\ \ldots,\ k-1;\quad v = k \end{cases} \tag{13}$$

The diagonal terms of the elastic component matrices $\mathbf{K}_{\mathrm{uv}}^{\mathrm{ik}}$ (for $u = v$) are expressed as

$$\mathbf{K}_{uv}^{ik} = \begin{cases} k_{ik}\left(\frac{a_{ik}}{r_i}\right)^2\mathbf{I} & u = v = i \\ k_{ik}\mathbf{I} & u = v = i+1,\ \ldots,\ k-1 \\ k_{ik}\left(\frac{b_{ik}}{r_k}\right)^2\mathbf{I} & u = v = k \end{cases} \tag{14}$$

Each elastic component matrix $\mathbf{K}_{\mathrm{uv}}^{\mathrm{ik}}$ shows the quantity of the elastic effect of the spring S_{ik} between links u and v. The elastic potential energy of the spring affects only the links that it spans, the nonzero elements of $\mathbf{K}_{\mathrm{uv}}^{\mathrm{ik}}$ are within the range $i \le u,\ v \le k$.

2.2. Static balance of total SBM

The gravitational and elastic potential energies change with the relative angular displacement between links u and link v, as shown in Eq. (15). To keep the total potential energy unchanged regardless of the configuration of the manipulator, all component matrices between any two distinct links ($u \neq v$) must be zero matrices.

$$\theta_{uv} = \cos^{-1}(r_u^T r_v) \tag{15}$$

Because the gravitational and elastic potential energies both have the same form, the total potential energy [$\mathbf{T}_{uv}$] can be expressed as the sum of the gravity and elastic SBMs, and $\mathbf{T}_{uv}$ denotes the total component matrices, which represent total potential energies between links u and v.

The gravitational potential energy induces nonzero elements in the first row of $\mathbf{T}_{uv}$ (for $u = 1$) only. The associated spring S_{ik} (for $i = 1$) with nonzero elements in the first row is required to balance $\mathbf{G}_{uv}$ (for $u = 1$). Therefore, the first row of the total component matrices can be expressed as

$$\mathbf{T}_{1v} = \mathbf{G}_{1v} + \sum_N \mathbf{K}_{1v}^{1k} = 0 \quad v = 2, \ \dots, \ n \tag{16}$$

The gravitational component matrix includes the gravitational values of variable payloads. To calculate the balancing equation of $\mathbf{T}_{1v}$ as scalar, the ground-attached end of spring S_{1k} must be installed at angle α_{1k} = 90° or 270°, and the link-attached end must be installed at angle β_{1k} = 0° or 180°. Therefore, the rotation matrix $\mathbf{I}'$ can be ignored during the calculation. The elastic component matrices $\mathbf{K}_{\mathrm{uv}}^{1\mathrm{k}}$ of spring S_{1k} can be rearranged as

$$\mathbf{K}_{uv}^{1k} = \begin{cases} -k_{1k}A_{1k}\mathbf{I}' & u = 1; \quad v = 2, \ \dots, \ k-1 \\ -k_{1k}A_{1k}B_{1k}\mathbf{I}' & u = 1; \quad v = k \\ k_{1k}\mathbf{I} & u, \quad v = 2, \ \dots, \ k-1 \\ k_{1k}B_{1k}\mathbf{I} & u = 2, \ \dots, \ k-1; \quad v = k \end{cases} \tag{17}$$

where A_{1k} and B_{1k} are determined to represent dimensionless installation parameters expressed as

$$A_{1k} = \frac{a_{1k}}{x_1}\sin(-\alpha_{1k}) = a_{1k}\sin(-\alpha_{1k}) \tag{18a}$$

$$B_{1k} = \frac{b_{1k}}{r_k}\cos(\beta_{1k}) \tag{18b}$$

The design parameters of spring S_{1k} include one spring constant k_{1k} and two installation parameters A_{1k} and B_{1k}. The installation parameter B_{1k} is fitted in both first-row and non-first-row component matrices, and it is attached to the non-ground link. Therefore, the adjustment of B_{1k} would additionally influence the non-first-row component matrices and interfere with the motion of links. However, the installation parameter A_{1k} is fitted in first-row component matrices only and is attached to the ground. Therefore, the adjustment of A_{1k} can avoid these problems. Thus, the installation parameter A_{1k} is known to be adjustable for variable payloads.

For the non-first-row elements of $\mathbf{T}_{uv}$ (for $u \neq 1$), gravity has no influence but the ground-adjacent springs have elastic influence. Therefore, spring S_{ik} (for $i \neq 1$) must be installed to generate a counterbalancing force in the non-first-row parts to compensate for the influence of the nonzero elements of $\mathbf{K}_{\mathrm{uv}}^{1\mathrm{k}}$ (for $u \neq 1$).

$$\mathbf{T}_{uv} = \sum_{\mathbf{N}} \mathbf{K}_{uv}^{1k} + \sum_{\mathbf{N}} \mathbf{K}_{uv}^{ik} = 0 \quad u, v \neq 1\ ;\ and\ \ i \neq 1 \tag{19}$$

Similarly, because the attachment angle of component matrix $\mathbf{K}_{\mathrm{uv}}^{\mathrm{ik}}$ (for $i \neq 1$) is defined as β_{1k} = 0° or 180°, the attached end of the counterbalancing spring S_{ik} should be installed at angles α_{1k} = 0° or 180° and β_{1k} = 0° or 180°, so the rotation matrix $\mathbf{I}$ can be ignored during the calculation. The elastic component matrices $\mathbf{K}_{\mathrm{uv}}^{\mathrm{ik}}$ of the counterbalancing spring S_{ik} can be rearranged as

$$\mathbf{K}_{uv}^{ik} = \begin{cases} -k_{ik}A_{ik}\mathbf{I} & u = i; \quad v = i+1, \ \dots, \ k-1 \\ -k_{ik}A_{ik}B_{ik}\mathbf{I} & u = i; \quad v = k \\ k_{ik}\mathbf{I} & u, \quad v = i+1, \ \dots, \ k-1 \\ k_{ik}B_{ik}\mathbf{I} & u = i+1, \ \dots, \ k-1; \quad v = k \end{cases} \tag{20}$$

where A_{ik} and B_{ik} are determined to represent dimensionless installation parameters as

$$A_{ik} = \frac{a_{ik}}{r_i}\cos(-\alpha_{ik}) \tag{21a}$$

$$B_{ik} = \frac{b_{ik}}{r_k}\cos(\beta_{ik}) \tag{21b}$$

In conclusion, the installation parameters are separated into three types according to their balancing objectives and positions. For a ground-adjacent spring, the ground-attached installation parameter A_{1k} is a PDP, and the link-attached installation parameter B_{1k} is a distal PIP. For a non-ground-adjacent spring, the installation parameter A_{ik} is a proximal PIP, and B_{ik} is a distal PIP. The

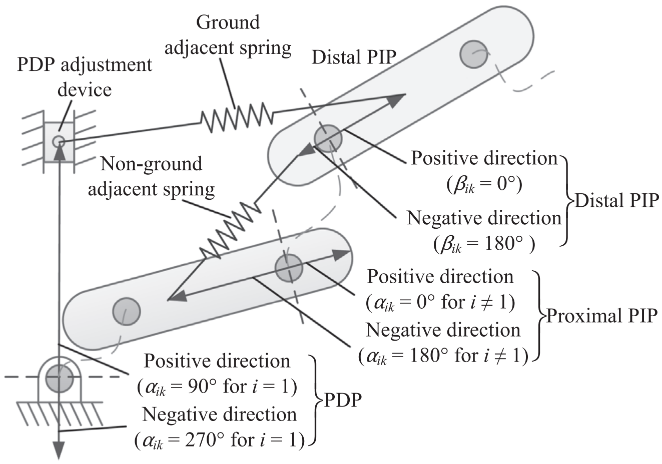

Fig. 2. Definitions of the directions of PDPs, proximal PIPs, and distal PIPs; schematic of a PDP adjustment device.

positive and negative directions of the PDPs and PIPs are determined as (90°, 270°) and (0°, 180°), respectively, as shown in Fig. 2. In addition, to enable adjustment, the PDPs must fit on PDP adjustment devices. PDP adjustment devices are used to adjust PDPs, and they can be locked at any position along the vertical axis, as shown in Fig. 2.

3. Determination PDP and PIP arrangements

3.1. Arrangement of PDPs

According to Sections 2.2, only ground-adjacent springs contain PDPs. In this section, the characteristics of PDPs are obtained by analyzing the equations of the first row of the total SBM [$\mathbf{T}_{uv}$]. To increase the efficiency of the adjustment when a payload is changed, the PDP terms should form a linear equation that is linear with respect to the change of payload. For a set of balancing equations with linear solutions, the number of unknowns must be equal to the number of subsets of equations. To enable the set of PDPs of the form A_{1k} to be adjustable for variable payloads m_p, A_{1k} is determined to be unknown for the simultaneous equations of the entries in the first row.

The balancing equations of the first row component matrices of $\mathbf{T}_{uv}$ contain $(n-1)$ component matrices, $\mathbf{T}_{12}$ to $\mathbf{T}_{1n}$. Therefore, $(n-1)$ equations are in the first row. For each fitted spring S_{1k}, one distinct unknown of PDP A_{1k} is added to the system. A total of $(n-1)$ springs should be connected to link 1; therefore, the total component matrices $\mathbf{T}_{1v}$ (for v = 2, ..., n) can be rearranged as

$$\mathbf{T}_{1v} = \mathbf{G}_{1v} + \sum_{k=2}^{n} \mathbf{K}_{1v}^{1k} = \begin{cases} \left(-g(m_p + W_v) - k_{1v}A_{1v}B_{1v} - \sum_{j=v+1}^{n} k_{1j}A_{1j}\right)\mathbf{I}' = 0 & v = 2, \ \ldots, \ n-1 \\ (-g(m_p + W_n) - k_{1n}A_{1n}B_{1n})\mathbf{I}' = 0 & v = n \end{cases} \tag{22}$$

All component matrices in Eq. (22) have the same orientation. Consequently, subset equations can be solved regardless of the orientation. The subset equations have the form of a first-order linear system. Therefore, Eq. (22) can be expressed as the matrix form of a linear system.

$$\begin{bmatrix} -k_{12}B_{12} & -k_{13} & \cdots & -k_{1v} & \cdots & -k_{1n} \\ 0 & -k_{13}B_{13} & -k_{14} & \cdots & \cdots & -k_{1n} \\ \vdots & & \ddots & & & \vdots \\ \vdots & & & \ddots & & \vdots \\ \vdots & & & & \ddots & -k_{1n} \\ 0 & \cdots & \cdots & \cdots & 0 & -k_{1n}B_{1n} \end{bmatrix} \begin{bmatrix} A_{12} \\ A_{13} \\ \vdots \\ \vdots \\ \vdots \\ A_{1n} \end{bmatrix} = \begin{bmatrix} gm_p + W_2 \\ gm_p + W_3 \\ \vdots \\ \vdots \\ \vdots \\ gm_p + W_n \end{bmatrix} \tag{23}$$

The solutions of PDP A_{1k} (for k = 2, ..., n) can be arranged as a subset of the linear equations of payloads, which can be expressed as

$$A_{1k} = C_k m_p + D_k \quad for \quad k = 2, \ \ldots, \ n \tag{24}$$

where C_k is the coefficient of the payload, which represents the displacement of the PDP according to the payload, and D_k is the constant of the PDP, which represents the initial position of the PDP. In addition, D_k is determined by the constants of PDPs succeeding it. C_k and D_k can be expressed as

$$C_k = -\frac{g}{k_{1k}B_{1k}} \prod_{j=k+1}^{n} \left(1 - \frac{1}{B_{1j}}\right) for \ \ k = 2, \ \ldots, \ n \tag{25a}$$

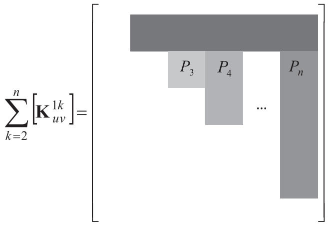

Fig. 3. Distribution features of the summations of the elastic SBM terms of ground-adjacent springs.

$$D_k = \begin{cases} -\frac{1}{k_{1n}B_{1n}}W_n & k = n \\ -\frac{1}{k_{1k}B_{1k}}\left(W_k - \sum_{j=k+1}^{n} k_j D_j\right) & k = 2, \ \dots, \ n-1 \end{cases} \tag{25b}$$

According to Eq. (25a–b), the PDPs are separated into two sets. The first set is used to balance the gravitational potential energy of variable payloads m_p. The second set is used to balance the constant gravitational potential energy of the links. Thus, the configuration of ground-adjacent springs has the characteristic CH1.

CH1: For an n-link VPM, $(n - 1)$ PDPs are used to compensate for the variations in the potential energies owing to changes in the payload. These PDPs are linear functions of the payload and can be formed by installing $(n - 1)$ ground-adjacent springs; that is, (for all $k = 2, \dots, n$) S_{1k} of an $n \times n$ spring configuration matrix is nonzero.

3.2. Arrangement of PIPs

The spring embedded between the ground and the end link produces nonzero terms in all components of the elastic SBM. However, only the terms in the first row are used to compensate for the gravitational potential energies; the other terms are excess elastic potential energies that are compensated by non-ground-adjacent springs.

Before installing non-ground-adjacent springs, it is necessary to identify the distribution of excess elastic potential energies in the relevant elastic SBM. According to **CH1**, ground-adjacent springs S_{12} to S_{1n} are installed, and the sum of their non-first-row elastic SBM terms has the same equations in the same column, as shown in Fig. 3 and Eq. (26). P_v (for $v = 3, \dots, n$) represents the excess elastic potential energies of the ground-adjacent springs in column v.

$$\mathbf{P}_k = \begin{cases} \sum_{j=2}^{n}\mathbf{K}_{2k}^{1j} = \cdots = \sum_{j=2}^{n}\mathbf{K}_{(k-1)k}^{1j} = \left(k_{1k}B_{1k} + \sum_{j=k+1}^{n} k_{1j}\right)\mathbf{I} = 0 & k = 3, \ \dots, \ n-1 \\ \sum_{k=2}^{n}\mathbf{K}_{2n}^{1k} = \cdots = \sum_{k=2}^{n}\mathbf{K}_{(n-2)n}^{1k} = \sum_{k=2}^{n}\mathbf{K}_{(n-1)n}^{1k} = (k_{1n}B_{1n})\mathbf{I} = 0 & k = n \end{cases} \tag{26}$$

According to Eq. (26), the excess elastic potential energies between column 3 and column $(n - 1)$ can be balanced by setting the distal PIPs B_{1k} (for $k = 3, \dots, n$) to negative values that can be formed by setting their distal attachment angles $\beta_{1k} = 180°$. However, because of the constraint that B_{1n} cannot equal zero, spring S_{2n} must be installed to compensate for the excess elastic potential energies in column n. Therefore, the installation of spring S_{2n} entails the characteristic CH2.

CH2: For an n-link VPM, a spring must be connected between link 2 and link n to compensate for the excess potential energies between link n and the links preceding it; that is, S_{2n} of an $n \times n$ spring configuration matrix must be nonzero.

Therefore, after the installation of spring S_{2n}, the final column of the non-first-row total SBM can be rearranged as

$$\mathbf{T}_{un} = \begin{cases} \mathbf{P}_n + k_{2n}A_{2n}B_{2n}\mathbf{I} = (k_{1n}B_{1n} - k_{2n}A_{2n}B_{2n})\mathbf{I} = 0 & u = 2 \\ \mathbf{P}_n + k_{2n}B_{2n}\mathbf{I} = (k_{1n}B_{1n} + k_{2n}B_{2n})\mathbf{I} = 0 & u = 3, \ \dots, \ n-1 \end{cases} \tag{27}$$

If the distal PIP B_{1q} (where q denotes a number between 3 and n) is set as a positive value (i.e., distal attachment angle $\beta_{1q} = 0°$), spring S_{2q} must be installed, and its distal PIP B_{2q} must be set to a negative value (i.e., distal attachment angle $\beta_{2q} = 180°$) to compensate for the excess elastic potential energy. Therefore, the distal PIP of springs S_{1q} and S_{2q} (for $3 \le q \le n$) has characteristic CH3.

CH3: For an n-link VPM, if the distal PIP of S_{1q} is not attached in the negative direction of link q, a spring with a distal PIP attached in the negative direction is required to fit between links 2 and q (where q denotes a number between 3 and n).

If spring S_{2q} is not installed, column q of the non-first-row total SBM can be rearranged as

$$\mathbf{T}_{uq} = \left(k_{1q}B_{1q} + \sum_{j=q+1}^{n} k_{1j} + \sum_{j=q+1}^{N} k_{2j}\right)\mathbf{I} = 0 \quad u = 2, \ \dots, \ q-1; \ \ and \ \ 3 \le q \le n \tag{28}$$

If spring S_{2q}, is installed, column q of the non-first-row total SBM can be rearranged as

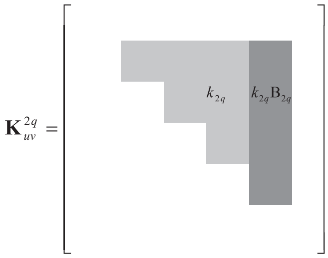

Fig. 4. Distribution features of nonzero terms in the elastic SBM with attachment point $a_{2q} = r_2$ and attachment angle $\alpha_{2q} = 180°$ (for $q > 3$).

$$\mathbf{T}_{uq} = \begin{cases} \left(k_{1q}B_{1q} + \sum_{j=q+1}^{n} k_{1j} - \sum_{j=q+1}^{N} k_{2j}A_{2j} - k_{2q}A_{2q}B_{2q}\right)\mathbf{I} = 0 & u = 2; \quad and \quad 3 \le q \le n \\ \left(k_{1q}B_{1q} + \sum_{j=q+1}^{n} k_{1j} + \sum_{j=q+1}^{N} k_{2j} + k_{2q}B_{2q}\right)\mathbf{I} = 0 & u = 3, \ \ldots, \ q-1; \quad and \quad 4 \le q \le n \end{cases} \tag{29}$$

where N denotes the number of springs that have been installed between link 2 and the links succeeding link q. For example, if springs S_{24} and S_{26} are installed, N = 4 and 6 should be considered in the balancing equations of $\mathbf{T}_{23}$.

According to Eqs. (27) and (29), after the installation of the springs connected between link 2 and the links succeeding link 2, the balancing equation in row 2 is different from those in the other rows. To solve the sequence of balancing equations without installing other springs S_{ik} (for $i \neq 1, 2$), each term in the same column should be the same as the term in its elastic SBM, and this can be achieved by setting its proximal PIP as $A_{2q} = -1$ (i.e., position $a_{2q} = r_2$ and attachment angle $\alpha_{2q} = 180°$). Therefore, the distribution features of the nonzero terms are as shown in Fig. 4. Note the following exceptional case: The elastic SBM of spring S_{23} is fitted in one field, it corresponds to one balancing equation only. Consequently, its proximal PIP A_{23} can be set at an arbitrary position.

Therefore, the sequence of balancing equations in column q of the non-first-row total SBM can be rearranged into a single equation as follows:

$$\mathbf{T}_{uq} = \begin{cases} \left(k_{13}B_{13} + \sum_{j=4}^{n} k_{1j} + \sum_{j=4}^{N} k_{2j} + k_{23}A_{23}B_{23}\right)\mathbf{I} = 0 & u = 2; \quad and \quad q = 3 \\ \left(k_{1q}B_{1q} + \sum_{j=q+1}^{n} k_{1j} + \sum_{j=q+1}^{N} k_{2j} + k_{2q}B_{2q}\right)\mathbf{I} = 0 & u = 2, \ \ldots, \ q-1; \quad and \quad 4 \le q \le n \end{cases} \tag{30}$$

The proximal PIP of spring S_{2q} (for $4 \le q \le n$) has the characteristic CH4.

CH4: For an n-link VPM, the proximal PIP of S_{2q} must be attached to joint 1 to compensate for the excess elastic potential energy without fitting non-ground- and non-link-2-adjacent springs; that is, S_{ik} (for $i, k \neq 1, 2$) of an $n \times n$ spring configuration matrix should be zero.

According to **CH1–4**, the spring configurations that can be applied for the VPM are

$$S_{ik} = \begin{cases} \# \quad (for \ \ i = 1, \ \ k = 2, \ \ \ldots, \ \ n) \\ \# \ or \ 0 \quad (for \ \ i = 2, \ \ k = 3, \ \ \ldots, \ \ n-1) \\ \# \quad (for \ \ i = 2, \ \ k = n) \\ 0 \quad (for \ \ i, \ \ k \neq 1, \ \ 2) \end{cases} \tag{31}$$

According to Eq. (31), the admissible spring configurations of 2-, 3-, and 4-DOF VPMs are derived and shown in Tables 1 (2-A), (3-A), (3-B), (4-A), (4-B), (4-C), and (4-D).

For a general arrangement with general displacement (i.e., the coefficients of PDPs are different), the number of required PDP adjustment devices is equal to the number of ground-adjacent springs, which is expressed as

$$N_p = n - 1 \tag{32}$$

An example of a 3-DOF VPM with five springs is derived. The spring configuration matrix contributed by five springs is denoted as (3-B) in Table 1. The balancing equations of the off-diagonal upper triangular portion of the total SBM can be derived accordingly. $\mathbf{T}_{12}$, $\mathbf{T}_{13}$, and $\mathbf{T}_{14}$ are the balancing equations of the gravitational and elastic potential energies, and $\mathbf{T}_{23}$, $\mathbf{T}_{24}$, and $\mathbf{T}_{34}$ are those of the excess potential energies.

$$\mathbf{T}_{12} = -W_2 - gm_p - k_{12}A_{12}B_{12} - k_{13}A_{13} - k_{14}A_{14} = 0 \tag{33a}$$

$$\mathbf{T}_{13} = -W_3 - gm_p - k_{13}A_{13}B_{13} - k_{14}A_{14} = 0 \tag{33b}$$

$$\mathbf{T}_{14} = -W_4 - gm_p - k_{14}A_{14}B_{14} = 0 \tag{33c}$$

$$\mathbf{T}_{23} = k_{13}B_{13} + k_{14} - k_{24}A_{24} - k_{23}A_{23}B_{23} = 0 \tag{33d}$$

$$\mathbf{T}_{24} = k_{14}B_{14} - k_{24}A_{24}B_{24} = 0 \tag{33e}$$

Table 1
Schematics of admissible arrangements of PDP adjustment devices for 2-, 3-, and 4-DOF VPMs.

2

$$\begin{bmatrix} 0 & \# & \# \\ & 0 & \# \\ & & 0 \end{bmatrix}$$

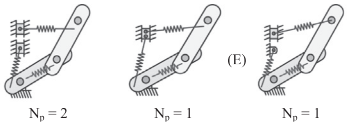

3

$$\begin{bmatrix} 0 & \# & \# & \# \\ & 0 & 0 & \# \\ & & 0 & 0 \\ & & & 0 \end{bmatrix}$$
(A)

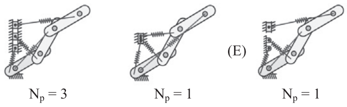

$$\begin{bmatrix} 0 & \# & \# & \# \\ & 0 & \# & \# \\ & & 0 & 0 \\ & & & 0 \end{bmatrix}$$
(B)

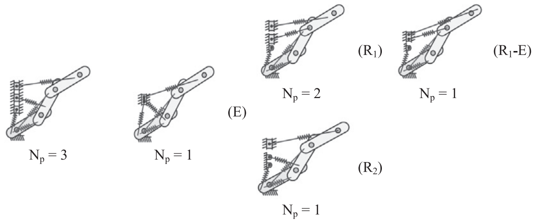

4

$$\begin{bmatrix} 0 & \# & \# & \# & \# \\ & 0 & 0 & 0 & \# \\ & & 0 & 0 & 0 \\ & & & 0 & 0 \\ & & & & 0 \end{bmatrix}$$
(A)

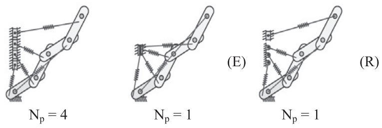

$$\begin{bmatrix} 0 & \# & \# & \# & \# \\ & 0 & \# & 0 & \# \\ & & 0 & 0 & 0 \\ & & & 0 & 0 \\ & & & & 0 \end{bmatrix}$$
(B)

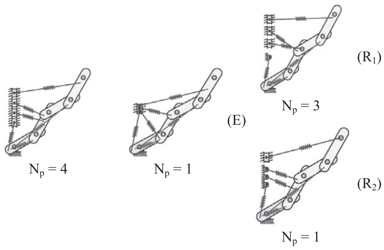

$$\begin{bmatrix} 0 & \# & \# & \# & \# \\ & 0 & 0 & \# & \# \\ & & 0 & 0 & 0 \\ & & & 0 & 0 \\ & & & & 0 \end{bmatrix}$$
(C)

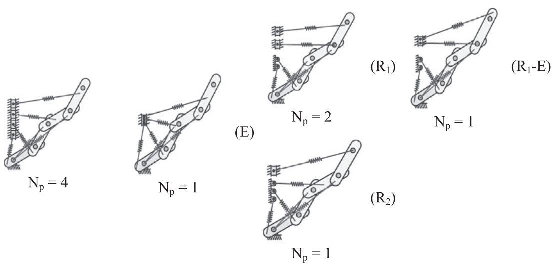

$$\begin{bmatrix} 0 & \# & \# & \# & \# \\ & 0 & \# & \# & \# \\ & & 0 & 0 & 0 \\ & & & 0 & 0 \\ & & & & 0 \end{bmatrix}$$
(D)

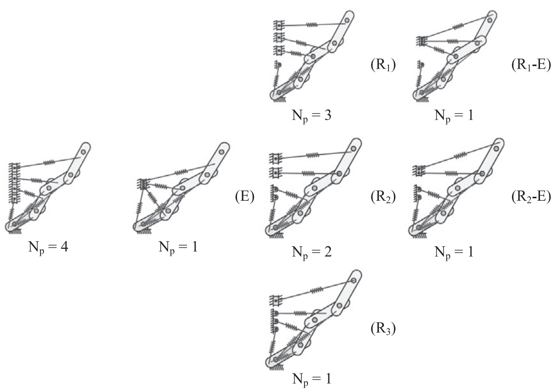

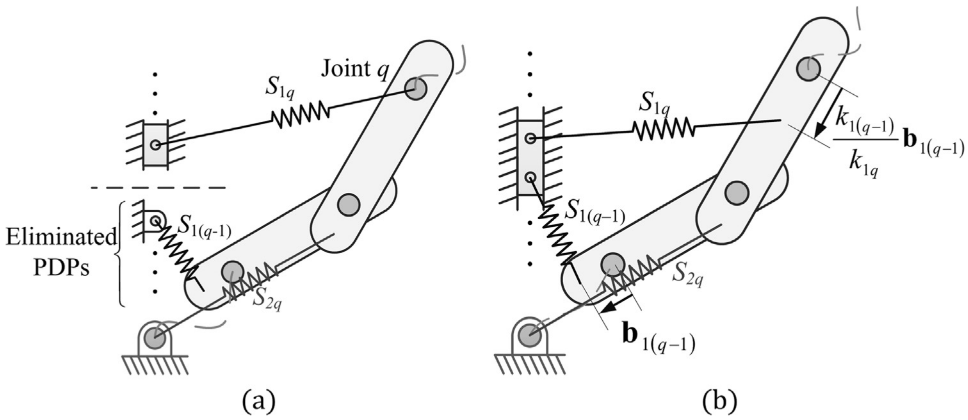

Fig. 5. Arrangements for reducing the number of PDP adjustment devices: (a) Reducing the number of PDPs; (b) Equivalent displacement of PDPs.

and

$$\mathbf{T}_{34} = k_{14}B_{14} + k_{24}B_{24} = 0 \tag{33f}$$

According to Eq. (33a–e) and **CH1–4**, the PDPs and PIPs can be expressed as

$$A_{14} = -\frac{g}{k_{14}B_{14}}m_p - \frac{1}{k_{14}B_{14}}W_4 \tag{34a}$$

$$A_{13} = -\frac{g}{k_{13}B_{13}}\left(1-\frac{1}{B_{14}}\right)m_p - \frac{1}{k_{13}B_{13}}\left(W_3 - \frac{1}{B_{14}}W_4\right) \tag{34b}$$

$$A_{12} = -\frac{g}{k_{12}B_{12}}\left(1-\frac{1}{B_{13}}\right)\left(1-\frac{1}{B_{14}}\right)m_p - \frac{1}{k_{12}B_{12}}\left(W_2 - \frac{1}{B_{13}}\left(W_3 - \frac{1}{B_{14}}W_4\right) - \frac{1}{B_{14}}W_4\right) \tag{34c}$$

$$B_{14} = -\frac{k_{24}}{k_{14}}B_{24} \tag{34d}$$

$$B_{13} = \frac{k_{23}A_{23}B_{23} - k_{14} - k_{24}}{k_{13}} \tag{34e}$$

and

$$A_{24} = -1 \tag{34f}$$

where B_{12}, B_{24}, A_{23}, and B_{23} are free variables that can be predetermined arbitrarily.

The general arrangement of the VPM is derived from the basic design equations of PDPs and PIPs. Because the number and displacements of PDPs are derived in general, $(n-1)$ PDP adjustment devices should adjust the system for A_{12} to A_{14} separately. However, some specific characteristics can reduce the number of PDP adjustment devices. This is discussed in the next section.

4. Minimal number of PDP adjustment devices

For the design of an n-link VPM, $(n-1)$ PDP adjustment devices are considered to be adjustable when the payload changes. As the number of PDPs increases, the adjustment of associated springs becomes more difficult. To avoid this situation, minimization of the number of PDP adjustment devices is discussed in this section.

4.1. Reduce the number of PDPs

According to Eq. (25a), $(1 - 1/B_{1q})$ is contained by a series of coefficients C_{1k} (for $k = 2, ..., q-1$). When $B_{1q} = 1$ (i.e., position $b_{1q} = r_q$ and angle $\beta_{1q} = 0°$), the coefficients C_{1k} of the PDPs preceding link q equal 0, and $(q-2)$ PDPs are then eliminated. Therefore, for a system with a reduced number of PDPs, the necessary condition CH5 applies.

CH5: For an n-link VPM, $(q-2)$ PDPs are eliminated by setting the distal PIP of S_{1q} attached at joint q (where q denotes a number between 3 and n).

However, **CH3** reveals that to set B_{1q} at joint q, a spring S_{2q} must be installed, and its distal PIP must be set at angle $\beta_{2q} = 180°$. A schematic of this arrangement is shown in Fig. 5(a).

For the general displacement, the number of PDP adjustment devices required is the same as the number of remaining PDPs, as expressed by

$$N_p = n - q + 1 \quad (If\ \ S_{2q} = \ \#, \ \ 3 \le q \le n) \tag{35}$$

The number of nonzero terms in the second row of the spring configuration matrix indicates the number of different arrangements for the reduced number of PDPs. With respect to the general arrangement, the arrangements for the reduced number of PDPs are shown in Table 1 with the symbol (R), as (2-A-R), (3-A-R), (3-B-R_1, R_2), (4-A-R), (4-B-R_1, R_2), (4-C-R_1, R_2), and (4-D-R_1, R_2, R_3).

4.2. Equivalent displacement of PDPs

For a VPM with more than one PDP, the equivalent displacement is designed to make the coefficients of the PDPs equal. Therefore, these PDPs can be set on the same PDP adjustment device. The equivalence equation of the coefficients of two adjacent PDPs is given as

$$C_q = C_{q-1} \quad 3 \le q \le n \tag{36}$$

By rearranging Eq. (36), the relationship between two distal PIPs B_{1q} and $B_{1(q-1)}$ is shown as

$$B_{1q} = \frac{k_{1(q-1)}}{k_{1q}} B_{1(q-1)} + 1 \quad 3 \le q \le n \tag{37}$$

Therefore, two adjacent PDPs can be fitted in the same PDP adjustment device so that they can be adjusted simultaneously; a schematic of this arrangement is shown in Fig. 5(b). For equalizing the displacements of adjacent PDPs, the necessary condition CH6 is applied.

CH6: For each pair of adjacent PDPs in an n-link VPM, the displacements of those two adjacent PDPs can be equalized by setting the distance between the distal PIP of S_{1q} and joint q as the product of the distal PIP of $S_{1(q-1)}$ and spring constant ratio of $S_{1(q-1)}$ and S_{1q} (for $3 \le q \le n$).

Because the displacements within each pair of adjacent PDPs can be equal, the displacements of all PDPs can be equalized by setting their distal PIPs in the relation expressed by Eq. (37). With respect to the general displacement, the arrangement for the equivalent displacement is shown in Table 1 with the symbol (E). The number of required PDP adjustment devices is minimized to one.

The arrangement of the combined method for **CH5** and **CH6** is valid. **CH5** reveals that an additional constraint ($B_{1q} = 1$) should be considered. To equalize the displacement of the remaining PDPs A_{1k} (for $k = q, ..., n$), their distal PIPs B_{1k} (for $k = q, ..., n$) should be greater than 1 (i.e., position $b_{1k} > r_k$ and distal attachment angle $\beta_{1k} = 0°$). Thus, springs S_{2k} (for $k = q+1, ..., n$) must be installed to ensure that the design is feasible.

The method of minimizing the number of PDPs is available for every situation. For the arrangement of a multi-PDP VPM with general displacement shown as (2), (3-A), (3-B), (3-2-R_1), (4-A), (4-B), (4-C), (4-C-R_1), (4-D), (4-D-R_1), and (4-D-R_2) in Table 1, their displacements can be equalized as shown in (2-E), (3-A-E), (3-B-E), (3-B-R_1-E), (4-A-E), (4-B-E), (4-C-E), (4-C-R_2-E), (4-D-E), (4-D-R_1-E), and (4-D-R_2-E), respectively. However, there is an exceptional case,(4-B-R_1): because spring $S_{24} = 0$, the displacement of A_{13} cannot be equal to the displacement of A_{14}. It is only for certain special conditions that the number of PDPs cannot be reduced to one.

According to **CH5** and **CH6**, the example of arrangement (3-B) shown in Section 3 can be redeveloped to reduce the number of required PDP adjustment devices. It is shown that arrangements (3-B-R_2), (3-B-E), and (3-B-R_1-E) require only one PDP adjustment device. Therefore, these three arrangements are derived as further examples.

For the arrangement (3-B-R_2), the additional constraint $B_{14} = 1$ should be considered. PDPs A_{12} and A_{13} are then eliminated, and Eq. (34a–f) can be rearranged as

$$A_{14} = -\frac{g}{k_{14}} m_p - \frac{1}{k_{14}B_{14}} W_4 \tag{38a}$$

$$A_{13} = -\frac{1}{k_{13}B_{13}} \left(W_3 - \frac{1}{B_{14}} W_4 \right) \tag{38b}$$

$$A_{12} = -\frac{1}{k_{12}B_{12}} \left(W_2 - \frac{1}{B_{13}} \left(W_3 - \frac{1}{B_{14}} W_4 \right) - \frac{1}{B_{14}} W_4 \right) \tag{38c}$$

$$B_{14} = 1 \tag{38d}$$

$$B_{13} = \frac{k_{23}A_{23}B_{23} - k_{14} - k_{24}}{k_{13}} \tag{38e}$$

$$A_{24} = -1 \tag{38f}$$

and

Table 2
Inertia and dimensional parameters of the 3-DOF manipulator.

j	m_j (kg)	r_j (m)	s_j (m)
2	0.162	0.2	0.07
3	0.162	0.2	0.07
4	0.122	0.15	0.053

$$B_{24} = -\frac{k_{14}}{k_{24}} \tag{38g}$$

where B_{12}, A_{23}, and B_{23} are free variables that can be predetermined arbitrarily.

For the arrangement (3-B-E), the equivalent displacements of PDPs can be derived on the basis of Eq. (37). Thus, the coefficients C_2, C_3, and C_4 are the same, and Eq. (34a–f) can be rearranged as

$$A_{14} = -\frac{g}{k_{14}B_{14}}m_p - \frac{1}{k_{14}B_{14}}W_4 \tag{39a}$$

$$A_{13} = -\frac{g}{k_{14}B_{14}}m_p - \frac{1}{k_{13}B_{13}}\left(W_3 - \frac{1}{B_{14}}W_4\right) \tag{39b}$$

$$A_{12} = -\frac{g}{k_{14}B_{14}}m_p - \frac{1}{k_{12}B_{12}}\left(W_2 - \frac{1}{B_{13}}\left(W_3 - \frac{1}{B_{14}}W_4\right) - \frac{1}{B_{14}}W_4\right) \tag{39c}$$

$$B_{24} = -\frac{k_{14}}{k_{24}}B_{14} \tag{39d}$$

$$B_{13} = \frac{k_{14}}{k_{13}}(B_{14} - 1) \tag{39f}$$

$$B_{12} = \frac{k_{13}}{k_{12}}(B_{13} - 1) \tag{39g}$$

$$A_{24} = -1 \tag{39h}$$

and

$$B_{23} = \frac{k_{13}B_{13} + k_{14} + k_{24}}{k_{23}A_{23}} \tag{39i}$$

where A_{23} and B_{14} are free variables that can be predetermined arbitrarily.

For the arrangement (3-B-R_1-E), $B_{13} = 1$ and Eq. (37) should be considered. PDP A_{12} is eliminated, and the coefficients C_3 and C_4 are the same. Eq. (34a–f) can be rearranged as

$$A_{14} = -\frac{g}{k_{14}B_{14}}m_p - \frac{1}{k_{14}B_{14}}W_4 \tag{40a}$$

$$A_{13} = -\frac{g}{k_{14}B_{14}}m_p - \frac{1}{k_{13}B_{13}}\left(W_3 + \frac{1}{B_{14}}W_4\right) \tag{40b}$$

$$A_{12} = -\frac{1}{k_{12}B_{12}}\left(W_2 + \frac{1}{B_{13}}\left(W_3 + \frac{1}{B_{14}}W_4\right) + \frac{1}{B_{14}}W_4\right) \tag{40c}$$

Table 3
Associated spring constants and attachment angles.

(a) 3-B-R_2 arrangement				(a) 3-B-E arrangement			(a) 3-B-R_1-E arrangement		
ik	k_{ik}(N/m)	α_{ik}(°)	β_{ik} (°)	k_{ik} (N/m)	α_{ik}(°)	β_{ik}(°)	k_{ik}(N/m)	α_{ik}(°)	β_{ik}(°)
12	300	270	180	300	90	180	100	270	180
13	200	270	180	100	90	180	25	90	0
14	100	90	0	100	90	0	100	90	0
23	300	180	180	300	180	180	600	180	180
24	200	180	180	200	180	180	300	180	180

Table 4
Installation parameters corresponding to different payloads.

(a) 3-B-R_2 arrangement

m_p(kg)	a_{12}(m)	a_{13}(m)	a_{14}(m)	a_{23}(m)	a_{24}(m)	b_{12}(m)	b_{13}(m)	b_{14}(m)	b_{23}(m)	b_{24}(m)
0	0.108	0.017	0.004	0.3	0.2	0.04	0.075	0.15	0.1	0.075
1			0.102							
2			0.2							
3			0.298							
d(m/kg)			0.098							

(b) 3-B-E arrangement

m_p(kg)	a_{12}(m)	a_{13}(m)	a_{14}(m)	a_{23}(m)	a_{24}(m)	b_{12}(m)	b_{13}(m)	b_{14}(m)	b_{23}(m)	b_{24}(m)
0	−0.075	−0.062	0.005	0.3	0.2	0.08	0.04	0.12	0.124	0.06
1	0.048	0.061	0.128							
2	0.171	0.184	0.251							
3	0.294	0.307	0.374							
d(m/kg)	0.123	0.123	0.123							

(c) 3-B-R_1-E arrangement

m_p(kg)	a_{12}(m)	a_{13}(m)	a_{14}(m)	a_{23}(m)	a_{24}(m)	b_{12}(m)	b_{13}(m)	b_{14}(m)	b_{23}(m)	b_{24}(m)
0	0.04	0.057	0.003	0.3	0.2	0.08	0.2	0.188	0.094	0.063
1		0.135	0.081							
2		0.213	0.159							
3		0.291	0.237							
d(m/kg)		0.078	0.078							

$$B_{14} = 1 + \frac{k_{13}}{k_{14}} B_{13} \tag{40d}$$

$$B_{13} = 1 \tag{40e}$$

$$B_{24} = -\frac{k_{14}}{k_{24}} B_{14} \tag{40f}$$

$$A_{24} = -1 \tag{40g}$$

and

$$B_{23} = \frac{k_{13} + k_{14} + k_{24}}{k_{23} A_{23}} \tag{40h}$$

where A_{23} and B_{12} are free variables that can be predetermined arbitrarily.

Eqs. (38a–g, 39a–i, and 40a–h) reveal that three arrangements of PDPs and PIPs can minimize the number of PDP adjustment devices through the associated installation constraints. On the basis of the specific requirements of different applications, suitable associated arrangements can be selected accordingly.

5. Illustrative examples of 3-DOF, five-spring VPM with a minimal number of PDP adjustment devices

We refer to the examples shown in Section 4. Three arrangements with minimal numbers of PDP adjustment devices are considered as illustrative examples. The inertia and dimensional parameters of the manipulator are shown in Table 2.

The spring constants k_{12}, k_{13}, k_{14}, k_{23}, and k_{24} are determined through trial and error with appropriate installation parameters A_{12}, B_{12}; A_{13}, B_{13}; A_{14}, B_{14}; A_{23}, B_{23}; and A_{24}, B_{24}. According to Eqs. (18a–b and 21a–b), A_{ik} and B_{ik} can be transformed into scalars a_{ik}, b_{ik} and angles α_{ik}, β_{ik}, which represent the distance and direction relative to the associated origin of each link. Their associated spring constants and attachment angles are listed in Table 3 (a)–(c).

Table 4 (a)–(c) shows the installation parameters corresponding to payloads of 0–3 kg. The PDPs change according to the payload, and the PIPs are independent of the payload. In addition, d is the displacement of the PDPs. In Table 4 (b), PDPs with negative values denote that they have been adjusted in the negative direction.

On the basis of Table 4, the installation parameters associated with payloads of 1 and 2 kg are illustrated in Fig. 6(a)–(c), respectively. The illustrated plots show proportions that are realistic with respect to the link lengths. The PDP adjustment devices in the schematic show that the joint is adjustable according to the displacement d as the payload changes, and it can be locked at a

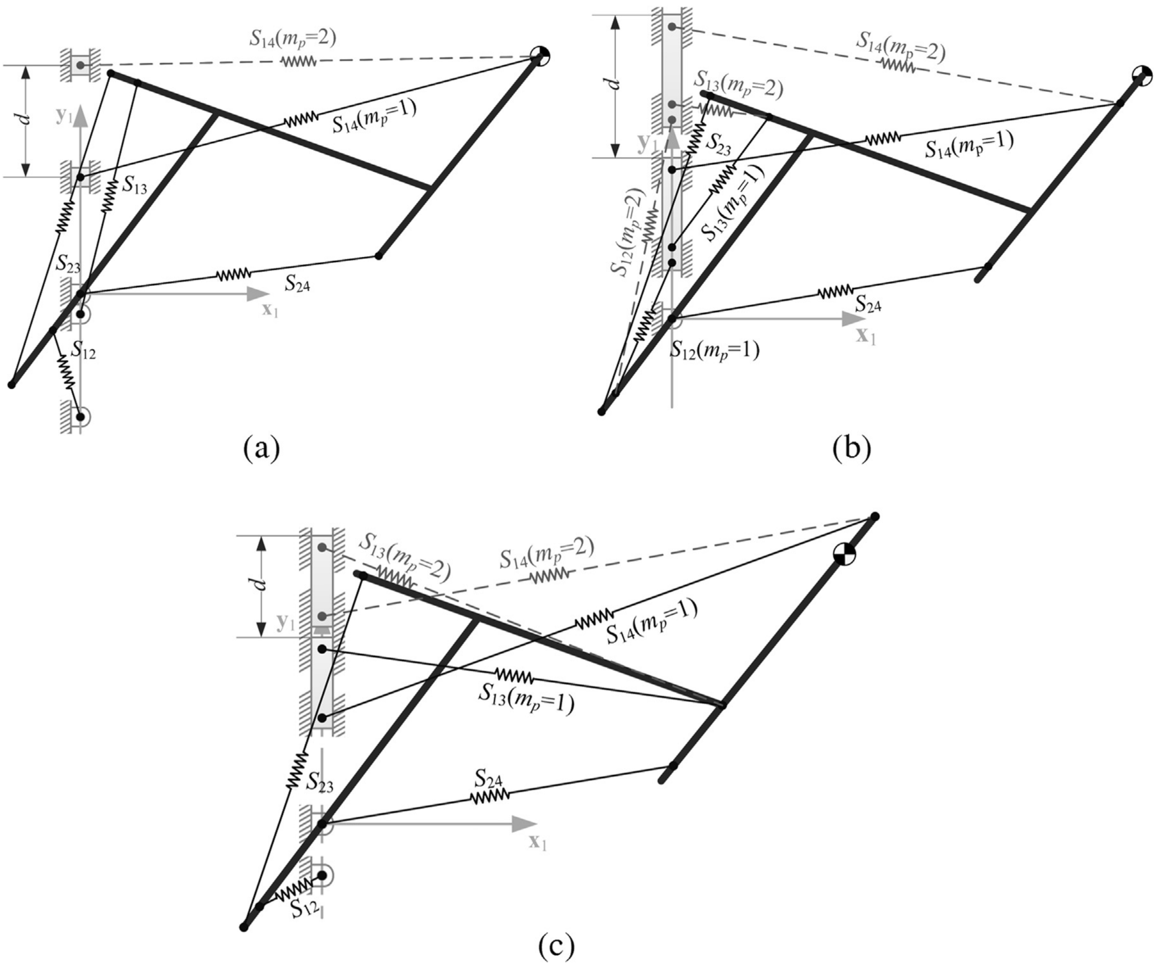

Fig. 6. Three-DOF, five-spring VPM with the minimal number of PDP adjustment devices with payloads of 1 and 2 kg: (a) 3-B-R_2 arrangement; (b) 3-B-E arrangement; (c) 3-B-R_1-E arrangement.

determined position along the vertical axis when the manipulator is functioning.

Three models were simulated using MATLAB® software, and the elastic potential energy functions and the gravitational potential energy functions with payloads of 1, 2, and 3 kg are plotted in Fig. 7(a)–(c). The motion initially has the orientations θ_2 = 90°, θ_3 = 0°, and θ_4 = 0°. Subsequently, links 2, 3, and 4 are lowered to complete the motion, where θ_2 = -30°, θ_3 = 60°, and θ_4 = 60°. The elastic and gravitational potential energies are transferred completely, and therefore, the simulated results of the total potential energy remain constant, as shown in Fig. 7. The total potential energy of each arrangement is shown in Table 5 respectively. The simulated results confirm that the three VPM designs with the minimal numbers of PDP adjustment devices can be balanced with different payloads and any configuration.

In Table 5, the column of ΔU^t represents energy required during movement of a PDP adjustment device from location of (m_p– 1) to location of m_p. The energy requirement ΔU^t increases when the payload increases. The energy consumption levels of arrangement 3-B-R_2 and 3-B-R_1-E are approximately equal. Arrangement 3-B-E requires less energy than arrangements 3-B-R_2 and 3-B-R_1-E for values of m_p between 0 and 1. However, the energy consumption levels for values of m_p between 1 and 2, and for values of m_p between 2 and 3 are apparently greater than the energy consumption levels of the other two arrangements. In summary, the energy efficiency levels for arrangements 3-B-R_2 and 3-B-R_1-E are similar. Arrangement 3-B-E performs more efficiently when the payload is less than 1 kg.

To change the payload and to move the PDP adjustment device without locking weight arms, the procedure should follow the steps as shown in Fig. 8(a)-(f). First, lower the payload to the ground so the links do not fall down when the PDP adjustment device is moved to the zero position (i.e., the position where m_p = 0). Remove the payload at the zero position, then the manipulator will maintain equilibrium. Second, put a new payload on the end link and set the PDP adjustment device to a new balanced position. At this point, the new payload is equilibrated.

To implement zero-free-length springs with high values of elongation, wire and pulley arrangements are needed for standard springs to emulate zero-free length springs [10]. The implementation of a wire and pulley arrangement for 3-B-R_2 is shown in Fig. 9. Spring S_{14} is fitted on the PDP adjustment device to adjust PDP values when the payload changes. Springs S_{12} and S_{13} are ground-

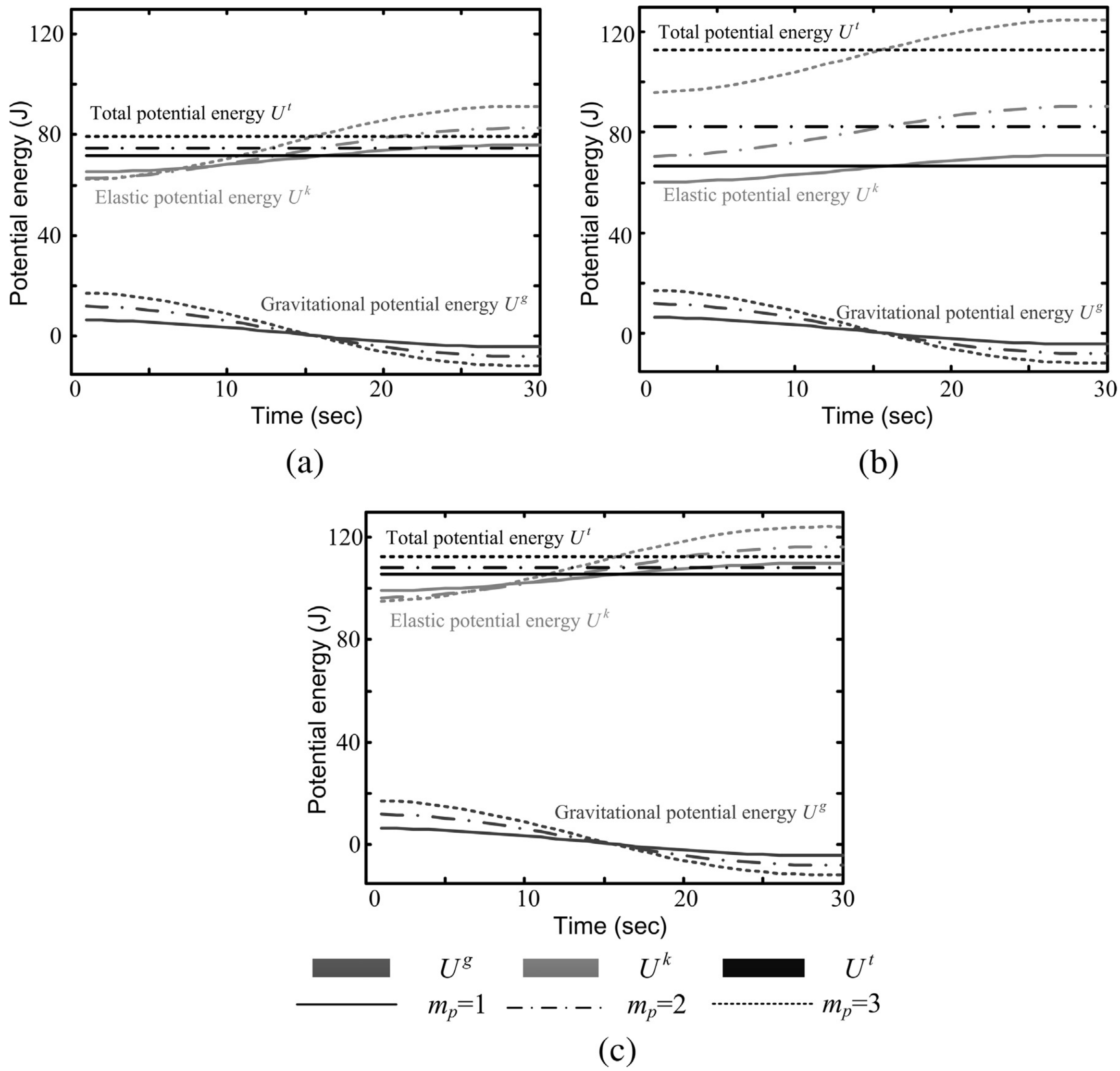

Fig. 7. Simulated potential energy values with payloads of 1, 2, and 3 kg: (a) 3-B-R_2 arrangement; (b) 3-B-E arrangement; (c) 3-B-R_1-E arrangement.

adjacent springs; hence, they can be guided to the ground directly. Springs S_{23} and S_{24} are non-ground-adjacent springs, therefore they should be guided to the origin point before the payload is set on the ground.

6. Conclusion

This paper presents a design methodology for determining the admissible arrangements of PDPs for different spring configurations. The balancing object of each installation parameter in the SBM is discussed according to its balancing equations. The ground-adjacent installation parameters are determined to be PDPs; PDPs are arranged to avoid the interference of the motion

Table 5
Total potential energy values with payloads of 0, 1, 2, and 3 kg, and the energy consumption values for adjusting PDPs to gain 1 kg of payload.

(a) 3-B-R_2 arrangement			(b) 3-B-E arrangement		(c) 3-B-R_1-E arrangement	
m_p (kg)	U^t (J)	ΔU^t (J)	U^t (J)	ΔU^t (J)	U^t (J)	ΔU^t (J)
0	70.533		65.933		104.528	
1	71.577	1.044	66.588	0.655	105.572	1.044
2	74.546	2.969	82.280	15.692	108.156	2.584
3	79.439	4.894	113.009	30.729	112.281	4.124

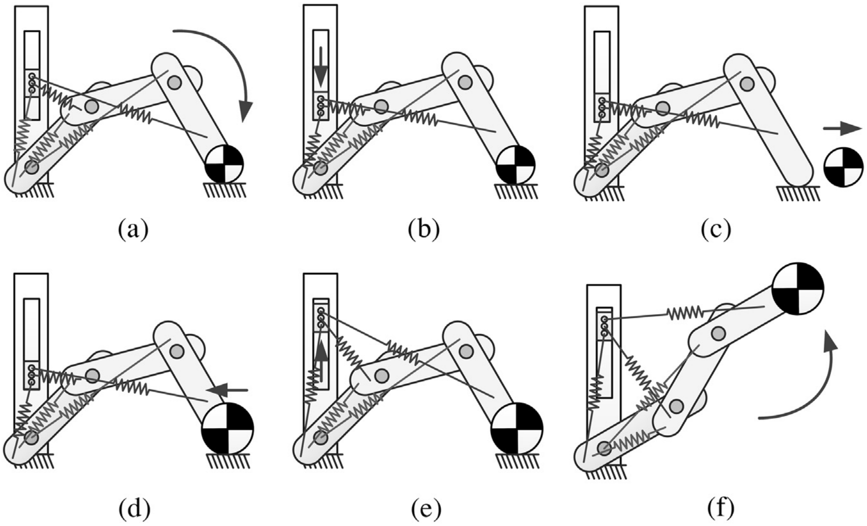

Fig. 8. Procedure for changing payloads and moving PDP adjustment device: (a) Lower the payload to the ground; (b) Return the PDP adjustment device to zero position; (c) Remove the payload; (d) Put on new payload; (e) Set the PDP adjustment device to new balanced position; (f) Lift new payload.

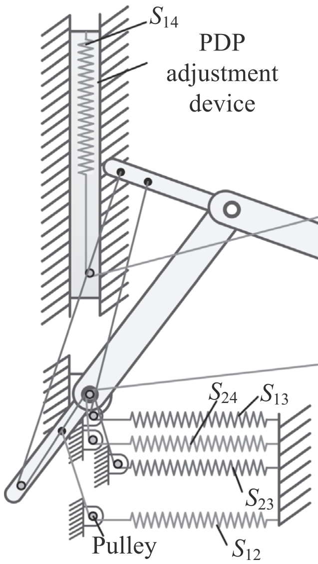

Fig. 9. Implementation of a wire and pulley arrangement for 3-B-R_2.

of links. The admissible spring configuration for a VPM is determined by the number of PDPs required to solve the simultaneous balancing equations. The derived equations of the PDPs are linear to the payload quantity. The PDP adjustment devices are sliders that can adjust the PDPs by movement to different positions; they can be locked at any position along the vertical axis. Thus, the number of PDP adjustment devices is determined by the number of PDPs. According to the interrelations between the PDPs and the PIPs, the minimal number of PDP adjustment devices is derived on the basis of two additional criteria: (1) reduction in the number of PDPs and (2) equivalent displacement of PDPs; thus, the required number of PDP adjustment devices can be minimized to one except for a few special situations. Three designs for a 3-DOF, five-spring VPM with the minimal number of PDP adjustment devices are used as illustrative examples. Each design has a specific arrangement of installation parameters, and the proper arrangement can be selected according to the requirements of each task. MATLAB computer simulation results are used to verify the static balance of different payload quantities, and the energy that the adjustments required were estimated accordingly.

References

[1] M. Walker, K. Oldham, A general theory of force balancing using counterweights, Mech. Mach. Theory 13 (1978) 175–185.
[2] M. Walker, R. Haines, An experimental study of the effects of counterweights on a six-bar chain, Mech. Mach. Theory 17 (1982) 355–360.
[3] E. Raghu, A. Balasubramonian, Experimental study on the elastodynamic behavior of the unbalanced and the counterweighted four bar mechanisms, J. Mech. Des. 112 (1990) 271–277.

[4] A. Martini, M. Troncossi, A. Rivola, Elastodynamic effects of mass-balancing: experimental investigation of a four-bar linkage, Adv. Mech. Eng. 5 (2013) 949457.
[5] J.G. Wang, C.M. Gosselin, Static balancing of spatial three-degree-of-freedom parallel mechanisms, Mech. Mach. Theory 34 (1999) 437–452.
[6] A.Fattah and S.K.Agrawal, Gravity-balancing of classes of industrial robots, in *Robotics and Automation, 2006. ICRA 2006. Proceedings 2006 IEEE International Conference on*pp. 2872–2877, 2006.
[7] T. Laliberté, C.M. Gosselin, M. Jean, Static balancing of 3-DOF planar parallel mechanisms, Mechatron. IEEE/ASME Trans. 4 (1999) 363–377.
[8] I. Simionescu, L. Ciupitu, The static balancing of the industrial robot arms: part i: discrete balancing, Mech. Mach. theory 35 (2000) 1287–1298.
[9] I. Simionescu, L. Ciupitu, The static balancing of the industrial robot arms: part II: continuous balancing, Mech. Mach. theory 35 (2000) 1299–1311.
[10] S.R.Deepak and G.Ananthasuresh, Static balancing of spring-loaded planar revolute-joint linkages without auxiliary links, in: *Proceedings of the 14th National Conference on Machines and Mechanisms (NaCoMM09), NIT, Durgapur, India*, 2009.
[11] D. Streit, E. Shin, Equilibrators for planar linkages, J. Mech. Des. 115 (1993) 604–611.
[12] T. Rahman, R. Ramanathan, R. Seliktar, W. Harwin, A simple technique to passively gravity-balance articulated mechanisms, Trans.-Am. Soc. Mech. Eng. J. Mech. Des. 117 (1995) 655–657.
[13] S.K. Agrawal, G. Gardner, S. Pledgie, Design and fabrication of an active gravity balanced planar mechanism using auxiliary parallelograms, J. Mech. Des. 123 (2001) 525–528.
[14] S.K. Agrawal, A. Fattah, Gravity-balancing of spatial robotic manipulators, Mech. Mach. Theory 39 (2004) 1331–1344.
[15] S.K. Agrawal, A. Fattah, Design of an orthotic device for full or partial gravity-balancing of a human upper arm during motion, in: *Intelligent Robots and Systems, 2003.(IROS 2003). Proceedings. 2003 IEEE/RSJ International Conference on*, 2003, pp. 2841–2846.
[16] S.K. Agrawal, A. Fattah, Theory and design of an orthotic device for full or partial gravity-balancing of a human leg during motion, Neural Syst. Rehabil. Eng. IEEE Trans. 12 (2004) 157–165.
[17] A. Fattah, S.K. Agrawal, G. Catlin, J. Hammnett, Design of a passive gravity-balanced assistive device for sit-to-stand tasks, J. Mech. Des. 128 (2006) 1122–1129.
[18] I. Ebert-Uphoff, C. m M. Gosselin, T. Laliberte, Static balancing of spatial parallel platform mechanisms—revisited, J. Mech. Des. 122 (2000) 43–51.
[19] I. Ebert-Uphoff, K. Johnson, Practical considerations for the static balancing of mechanisms of parallel architecture, Proc. Inst. Mech. Eng. K: J. Multi-body Dyn. 216 (2002) 73–85.
[20] C. Baradat, V. Arakelian, S. Briot, S. Guegan, Design and prototyping of a new balancing mechanism for spatial parallel manipulators, J. Mech. Des. 130 (2008) 072305.
[21] M. Carricato, C. Gosselin, A statically balanced Gough/Stewart-type platform: conception, design, and simulation, J. Mech. Robot. 1 (2009) 031005.
[22] A. Martini, M. Troncossi, M. Carricato, A. Rivola, Static balancing of a parallel kinematics machine with Linear-Delta architecture: theory, design and numerical investigation, Mech. Mach. Theory 90 (2015) 128–141.
[23] I. Simionescu, L. Ciupitu, L.C. Ionita, Static balancing with elastic systems of DELTA parallel robots, Mech. Mach. Theory 87 (2015) 150–162.
[24] Y.-Y. Lee, D.-Z. Chen, Determination of spring installation configuration on statically balanced planar articulated manipulators, Mech. Mach. Theory 74 (2014) 319–336.
[25] P.-Y. Lin, Design of statically balanced spatial mechanisms with spring suspensions, J. Mech. Robot. 4 (2012) 021015.
[26] P.-Y. Lin, W.-B. Shieh, D.-Z. Chen, Design of statically balanced planar articulated manipulators with spring suspension, Robot. IEEE Trans. 28 (2012) 12–21.
[27] R. Nathan, A constant force generation mechanism, J. Mech., Transm., Autom. Des. 107 (1985) 508–512.
[28] B.M. Wisse, W.D. Van Dorsser, R. Barents, J.L. Herder, Energy-free adjustment of gravity equilibrators using the virtual spring concept, in: *Rehabilitation Robotics, 2007. ICORR 2007. IEEE 10th International Conference on*, 2007, pp. 742–750.
[29] W.D. Van Dorsser, R. Barents, B.M. Wisse, J.L. Herder, Gravity-balanced arm support with energy-free adjustment, J. Med. Dev. 1 (2007) 151–158.
[30] W. Van Dorsser, R. Barents, B. Wisse, M. Schenk, J. Herder, Energy-free adjustment of gravity equilibrators by adjusting the spring stiffness, Proc. Inst. Mech. Eng. C: J. Mech. Eng. Sci. 222 (2008) 1839–1846.
[31] R. Barents, M. Schenk, W.D. van Dorsser, B.M. Wisse, J.L. Herder, Spring-to-spring balancing as energy-free adjustment method in gravity equilibrators, J. Mech. Des. 133 (2011) 061010.
[32] N. Takesue, T. Ikematsu, H. Murayama, H. Fujimoto, Design and prototype of variable gravity compensation mechanism (VGCM), J. Robot. Mechatron. (2011).